Spatial Mapping of Ether Lipids in Tissue via MALDI TIMS Imaging Mass Spectrometry: Characterization of Biomarkers of Peroxisomal Disorders

Melanie J. Campbell,[1] Erin H. Seeley,[1] Wei Cui,[2] Ann B. Moser,[5,6] Nancy E. Braverman,[2,3,4] Jennifer S. Brodbelt[1]

[1] Department of Chemistry, The University of Texas at Austin, Austin, TX, USA; [2] Research Institute of the McGill University Health Center, [3] Department of Human Genetics, [4] Department of Pediatrics, McGill University, Montreal, Quebec, Canada; [5] Kennedy Krieger Institute, [6] School of Medicine, Johns Hopkins University, Baltimore, MD, USA

Overview

- Localize ether lipids in peroxisomal disorder brain tissue via matrix-assisted laser desorption/ionization (MALDI) imaging mass spectrometry (IMS)
- Utilize trapped ion mobility spectrometry (TIMS) to gain collisional-cross section information for ether lipids that are under-characterized in the field

Introduction

Rhizomelic chondrodysplasia punctata (RCDP) is a rare peroxisomal disorder that is characterized by a severe deficiency of vinyl ether glycerophospholipids[1], also known as plasmalogens, which play a critical role in myelin development and function. Previous reports show that myelination is abnormal in RCDP patients and is correlated to plasmalogen dysregulation.[2] In this study, a RCDP mouse model was created by mutating the gene that encodes for the peroxisomal protein transporter, Pex7; thus, preventing the transfer of alkyl-dihydroxyacetonephosphate synthase (AGPS), a key enzyme in the plasmalogen biosynthesis pathway, into the peroxisome (**Scheme 1**).[3] We previously combined liquid chromatography-mass spectrometry (LC-MS) with 213 nm ultraviolet photodissociation (UVPD) to identify and quantify ether lipids in the cerebellum, hippocampus, and cortex of this mouse model.[4] We aim to enhance our understanding of the spatial distribution of ether lipids within the brain tissue of RCDP-afflicted mice using matrix-assisted laser desorption/ionization (MALDI) imaging mass spectrometry (IMS). Additionally, we will utilize trapped ion mobility spectrometry (TIMS) to determine the collisional-cross sections (CCS) for plasmalogens that are currently under-characterized by ion mobility.

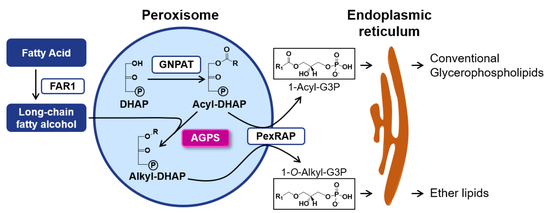

Scheme 1: Plasmalogen biosynthesis pathway where Pex7, a peroxisomal protein transporter responsible for the transfer of AGPS into the peroxisome, is disrupted.

Methods

Brain samples from Pex7$^{null/null}$ and Pex7 $^{WT/null}$ mice, provided by the Research Institute of McGill University Health Centre, were cryo-sectioned at a 12 µm thickness, thaw-mounted onto glass slides, and washed three times with cold ammonium formate (50 mM). The slides were heated to 50°C and coated with 10 mg/mL 1,5-diaminonaphthalene (DAN) in 70% acetonitrile using a HTX M5 sprayer. All experiments were performed in negative mode using a Bruker timsTOF fleX mass spectrometer. Tissue imaging data was acquired at 50 µm resolution with 200 shots per pixel. TIMS mode was used to obtain CCS (Å^2) values for the ether lipids (**Scheme 2**).

MALDI Imaging:

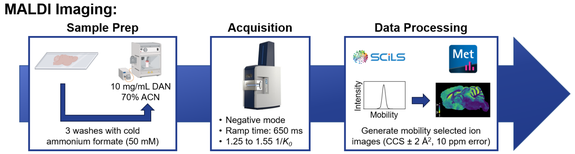

LC-MS Validation:

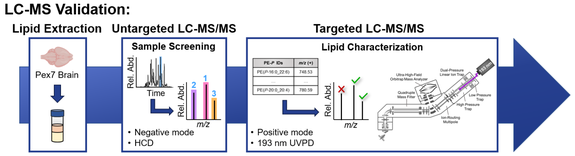

Scheme 2: Workflow for MALDI imaging and LC-MS validation. Created with BioRender.com.

Results and Discussion

Motivation:

Previously, we utilized LC-MS with 213 nm UVPD to identify and relatively quantify ether lipids in isolated regions of peroxisomal disorder mouse brain.[4] In the cerebellum and cortex of both control and Pex7 model mice, a total of 17 phosphatidylethanolamine (PE) plasmalogens were identified (**Figure 1**). The relative quantitation results confirmed the expected downregulation of PE plasmalogens in the Pex7 model. We aim to use these findings to guide our analysis of the control and Pex7 mouse brain when employing our MALDI-TIMS IMS workflow.

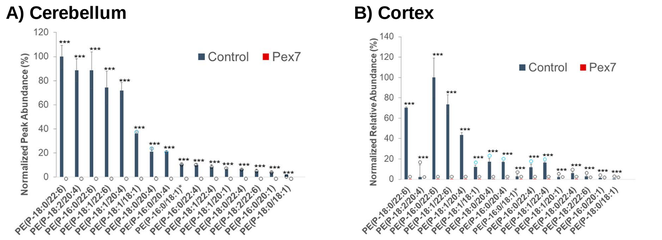

Figure 1: Normalized peak areas of identified ether lipids categorized by control and Pex7 mutation. Statistical significance is denoted by $p < 0.01$ (***) and $p < 0.05$ (**). Circles in blue, black, and red represent normalized abundances below LOQ, below LOD, and not detected, respectively. Adapted from Blevins, M.S.; Shields, S.W.J. *Anal. Chem.* **2022** *94* (37), 12621-12629

Imaging:

MALDI-TIMS IMS was performed on control and Pex7 brain tissue, revealing the distribution of 9 PE plasmalogens contrasted against lipids with opposing localization (**Figure 2**). Plasmalogens are absent in the Pex7 tissue, but insight into the spatial distribution of these lipids in healthy tissue can be discerned. For example, *m/z* 722.51, identified as PE(*P*-16:0/20:4) via LC-MS/MS analysis of the cortex, is the most abundant in the frontal lobe. LC-MS with 213 nm UVPD analysis identified PE(*P*-18:2/20:4) and PE(*P*-16:0/22:6) (*m/z* 746.51) in the cerebellum; however, the cerebellum contains both grey and white matter that serve critical, but different roles in the tissue. IMS localized these isomers (*m/z* 746.54) to the cerebellum's grey matter, providing further insight into their role in the brain.

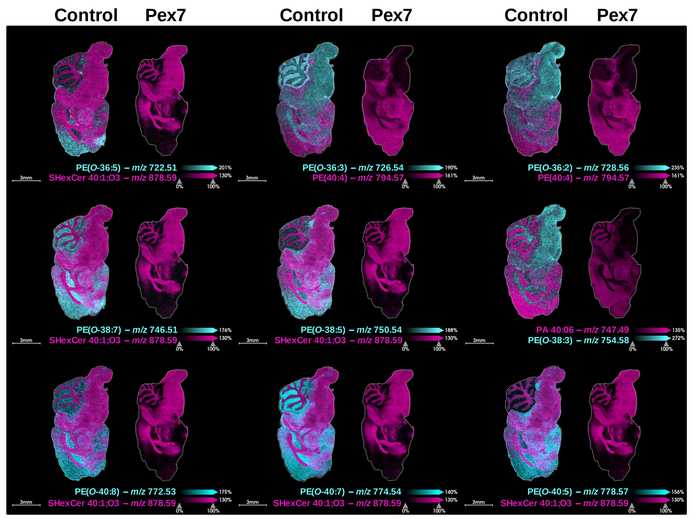

Figure 2: Ion mobility selected images (50 µm) for ether lipids identified via LC-MS/MS analysis with 10 ppm mass error. Ether lipids are displayed using a cyan heat map, while lipids with contrasting distributions are shown in pink.

The LC-MS workflow was developed to identify conventional and ether PE and PC lipids with an untargeted search followed by a separate run with UVPD for an in-depth, targeted characterization of ether lipids. While this method worked well for ether lipids, IMS unveiled the dysregulation of non-ether lipids more rapidly. **Figure 3** compiles the ion images of six lipids, identified with MetaboScape, that have differential distributions in the control and Pex7 tissue. These imaging results align with previous reports that PE 16:0/20:4 (*m/z* 738.50) was highly abundant in the cortex of the Pex7 model.[4] Further, other lipids, such as PI(38:4), that were not the focus of the LC-MS analysis were found to be dysregulated between these two tissue types. Future work aims to expand the untargeted LC-MS/MS workflow to identify a wide range of lipids that may impact the disease state and are currently being overlooked.

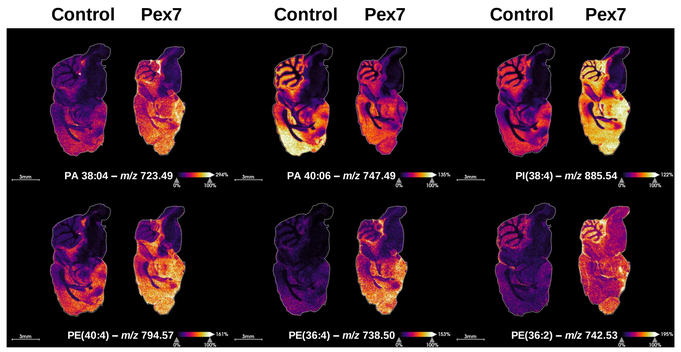

Figure 3: Ion mobility selected images (50 µm) for non-ether lipids that are dysregulated in Pex7 model. Lipids were identified via MetaboScape with less than a 10 ppm mass error.

By combining LC-MS with 193 nm UVPD and TIMS analysis, PE plasmalogens can be comprehensively characterized (**Figure 4**). TIMS was utilized to establish the CCS values for underreported lipids (**Figure 4A**). The LC-MS with 193 nm UVPD method not only determines the lipids retention time, but can also resolve the lipids identity down to the double bond position (**Figure 4B & 4C**). This data analysis workflow was performed for all PE plasmalogens identified by the LC-MS with 193 nm UVPD method and are presented in **Table 1**.

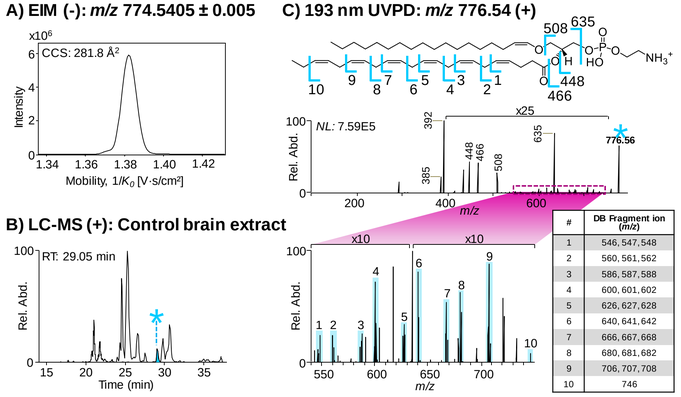

#	DB Fragment ion (*m/z*)
1	546, 547, 548
2	560, 561, 562
3	586, 587, 588
4	600, 601, 602
5	626, 627, 628
6	640, 641, 642
7	666, 667, 668
8	680, 681, 682
9	706, 707, 708
10	746

Figure 4: Comprehensive characterization of PE(*P*-18:0/22:6) combining **A)** extracted ion mobiligram (EIM) from TIMS analysis for CCS determination, **B)** LC-MS chromatography for retention time information, and **C)** 193 nm UVPD (8 pulses, 2.5 mJ/pulse) for structural identification. Double bond region is highlighted with a pink dashed box and magnified to show diagnostic ions.

Table 1: List of PE plasmalogens identified by LC-MS/193 nm UVPD and collision cross sections (CCS) determined by TIMS.

Theoretical *m/z* $[M-H]^-$ / $[M+H]^+$	Lipid ID by LC-MS	RT (min)	CCS (Å^2) N = 3
746.51 / 748.53	PE(*P*-18:2/20:4) PE(*P*-18:1/20:5) PE(*P*-16:0/22:6)	22.21 23.06 23.98	275.7 ± 0.6
722.51 / 724.53	PE(*P*-16:0/20:4)	24.85	271.7 ± 0.6
748.53 / 750.55	PE(*P*-18:1/20:4)	25.50	276.1 ± 0.6
750.54 / 752.56	PE(*P*-18:1/20:3) PE(*P*-16:0/22:4) PE(*P*-18:0/20:4)	27.53 28.67 30.21	277.9 ± 0.6
774.54 / 776.56	PE(*P*-18:0/22:6)	29.05	281.7 ± 0.6
700.53 / 702.54	PE(*P*-16:0/18:1) PE(*P*-18:1/16:0)	29.18	268.9 ± 0.7
726.54 / 728.56	PE(*P*-18:1/18:1) PE(*P*-18:0/18:2) PE(*P*-16:0/20:2)	29.80 30.77 30.77	273.2 ± 0.6
778.57 / 780.59	PE(*P*-18:0/22:4) PE(*P*-20:0/20:4)	34.45 36.16	283.8 ± 0.6
728.56 / 730.58	PE(*P*-16:0/20:1) PE(*P*-18:0/18:1)	34.61 35.04	275.4 ± 0.7
754.58 / 756.59	PE(*P*-18:1/20:1) PE(*P*-18:0/20:2)	35.37 36.16	279.9 ± 0.8

Conclusion

- Localized 9 PE plasmalogens to gain insight into the role they play in the mouse brain tissue of the peroxisomal disorder, RCDP
- Leveraged the information provided from combining LC-MS with 193 nm UVPD and MALDI-TIMS IMS to comprehensively characterize PE plasmalogens
- Determined CCS values for underreported ether lipids with TIMS analysis

References & Acknowledgements

(1) Braverman, N. E.; Moser, A. B. Functions of Plasmalogen Lipids in Health and Disease. *Biochim. Biophys. Acta BBA - Mol. Basis Dis.* 2012, *1822* (9), 1442–1452.

(2) Bams-Mengerink, A. M.; Majoie, C. B. L. M.; Duran, M.; Wanders, R. J. A.; Van Hove, J.; Scheurer, C. D.; Barth, P. G.; Poll-The, B. T. MRI of the Brain and Cervical Spinal Cord in Rhizomelic Chondrodysplasia Punctata. *Neurology* 2006, *66* (6), 798–803.

(3) Braverman, N.; Zhang, R.; Chen, L.; Nimmo, G.; Scheper, S.; Tran, T.; Chaudhury, R.; Moser, A.; Steinberg, S. A Pex7 Hypomorphic Mouse Model for Plasmalogen Deficiency Affecting the Lens and Skeleton. *Mol. Genet. Metab.* 2010, *99* (4), 408–416.

(4) Blevins, M. S.; Shields, S. W. J.; Cui, W.; Fallatah, W.; Moser, A. B.; Braverman, N. E.; Brodbelt, J. S. Structural Characterization and Quantitation of Ether-Linked Glycerophospholipids in Peroxisome Biogenesis Disorder Tissue by Ultraviolet Photodissociation Mass Spectrometry. *Anal. Chem.* 2022, *94* (37), 12621-12629.

THE Welch FOUNDATION · CPRIT · NSF · NIH

Follow us at @BrodSquadUT !